Techno-economic Evaluation of the Effects of Impurities on Conditioning and Transport of CO_2 by Pipeline

Geir Skaugen [a,*], Simon Roussanaly[a], Jana Jakobsen[a], Amy Brunsvold[a]
[a]*SINTEF Energy Research, Sem Sælandsvei 11, NO-7465 Trondheim, Norway*

* Corresponding author. Tel.: +47 9300 7154; fax: +47 735 97 250; E-mail address: geir.skaugen@sintef.no

Abstract

This study analyses the effect of transporting 13.1 MTPA CO_2 with impurities over a distance of 500 km on the operating and investment costs. In the cases study, two different impurity levels coming as a result of gas sweetening (GAS) and from capture from oxy-fuel combustion (OXY). The analysis includes the cost for the conditioning and the compression of the CO_2 stream after capture, from atmospheric conditions to transport conditions in the dense phase. In the calculation of the operating cost in terms of compression power and cooling requirements, the effect of the impurities are taken into account by using real thermo-physical properties depending of local fluid temperature and pressure and including heat transfer with the surroundings. The analysis investigates the total cost of choosing different pipeline diameters for transporting CO_2. The technical analysis shows that the number of required booster stations increases from 2 to 17 going from a 28" to an 18" pipeline and from 3 to 25 in the worst case with (GAS). In the second technical comparison, the feed flow rate for the CO_2 mixtures has been reduced so that the installed compression power for transport will be equal for all three cases. In this analysis a 24" pipeline with 4 booster stations was used.

The techno-economic assessments show a significant impact of the impurity cases considered on the CO_2 conditioning and transport design and cost. Indeed, in the Oxy-feed and Gas-feed cases, the specific conditioning and transport costs are respectively 13 and 22% higher than in the Base-feed case for the cost-optimal diameter. In absolute value, this represents a direct increase of the specific conditioning and transport cost of 2.3 and 3.8 €/$t_{CO2,avoided}$. Even if the cost evaluation leads to the same cost optimal diameter for the three impurity cases considered, it is important to note that this result is specific to the transport system considered in this paper and that in principle different impurity cases can lead to different cost-optimal diameters especially for low pipeline diameters.

The impact of impurities on an existing pipeline infrastructure design not taking into account these potential impurities show an even stronger cost impact. Indeed, the cost evaluations shows that the specific cost of the Oxy-feed and Gas-feed cases can be expected to be respectively at least around 20 and 40% more expensive than in the Base-feed case due to the lower amounts of CO_2 transported and the important cost-penalty associated with the CO_2 emissions not transported.

Finally, while the cost presented here considered only the impact of impurities on the conditioning and transport cost, impurities can also be expected to have a significant impact on the technical and economic performances of the whole CCS chain. This therefore highlights the importance of evaluating, on a case-to-case basis, the trade-offs between impact of impurities on the CCS cost and cost of impurities removal in order to provide recommendations on cost-optimal level of impurities along the chain.

Keywords: Pipeline transport, Effects of impurities, Thermodynamic, Energy consumption, pipeline safety, Techno-economic evaluation

Abbreviations: CCS, carbon capture and storage; CEPCI, chemical engineering plant cost index; GHG, greenhouse gas; IPCC, Intergovernmental Panel on Climate Change; NOAK, nth of a kind; ROW, right of way

1 Introduction

The rate of greenhouse gas emissions is continuing to accelerate with the growth of gross domestic product and population in spite of all efforts to reduce emissions. Delaying mitigation actions is expected to increase the difficulty of, and narrow the options for, limiting global warming to 2 °C (Climate change, 2014) There is currently general consensus regarding the role of CCS as a vital part of any greenhouse gas emission mitigation scenario, and the importance of CCS is widely acknowledged (Global Carbon Capture and Storage Institue, 2014) Furthermore, in its 2015 update, the above-mentioned institute demonstrated that without CCS, the reduction targets cannot be met and the costs of mitigating greenhouse gas emissions would be more than doubled (The Global CCS Institute, 2015).

The European Union has agreed on the 2030 targets of a 80-95% reduction in GHG emissions compared to 1990 levels, where a 40% greenhouse gas reduction target was set that is binding at nation-state level, and may not be met by carbon offsets and carbon capture and storage would need to deployed on a broad scale according to (European Climate Foundation, 2010) The United Nations Climate Change Conference (COP 21) in December 2015 adopted the Paris Agreement, whereby Parties agreed to "pursue efforts to" limit global temperature increase caused by anthropogenic climate change to 1.5 °C. The agreement calls for zero net anthropogenic greenhouse gas emissions to be reached during the second half of the 21st century. In spite of these positive developments with respect to global attitudes to CCS and the significant progress being made in CCS technologies, the momentum for the further development and deployment of CCS is slowing down, especially in Europe (IEA, 2014). The CCS technology is available and could be employed in the electricity generation sector as well as in industry, but investors and CCS stakeholders require confidence in earnings of sufficient size and duration if they are to become involved in CCS projects.

Techno-economic assessments that utilize fundamental knowledge of the thermo-physical properties of the CO_2 stream are crucial for the implementation of energy- and cost-efficient design of CO_2 transport and storage infrastructure. Studies on future European CO_2 transmission networks foresee more than 20000 km of pipeline by 2050 (Morbee et al., 2012), which will require full understanding of all aspects of CO_2 pipeline transport, from both technological and economic perspectives. Knoope et al. (2013) present a comprehensive state-of-the-art review of the various elements involved in analysing the costs of CO_2 pipeline transport. The main elements that are discussed are property models for CO_2 and cost models for the pipeline and booster stations, with special attention being paid to the variety of models for selecting the optimal pipeline diameter. Several knowledge gaps are identified, and the main concerns are that most of the published models are based on the costs of natural gas pipelines without any correction, and that none of the models includes the economic consequences of impurities in the CO_2 stream. Knoope et al. also points out that the CCS chain would need to be optimized simultaneously – noting particularly that the compression, pipeline and booster stations need to be linked to each other. Not specifically addressed in this review was the need to take fully into account the changes in physical properties along the pipeline – especially important when impurities are taken into account. This point is partly addressed by Witkowski et al. (2013), who demonstrated how varying ambient and soil temperatures will have significant effects on the cooling of the transported CO_2 and thus on its physical properties, flow velocities and pressure loss. These parameters can determine whether recompression is necessary or not. However, the analysis did not focus on the inclusion of impurities. Luo et al., (2014) link the compression, collecting pipelines, trunk pipeline and booster stations in their techno-economic evaluation of a transport pipeline network, analysing CO_2 with impurities from two specific emitters. Heat transfer between the transported fluid and the surroundings is either not included or is insignificant in their case, because the stream is already cooled to 20 °C before it enters the main trunk pipeline. A recent study (Zhao et al., 2016) emphasizes the importance of the varying ambient temperature on pressure loss and optimal pipeline design. However, their calculations were performed for pure CO_2, and it is not clear whether heat transfer mechanisms are included in the underlying models, while physical properties such as density and viscosity are based on the average temperature and pressure in the pipeline. Another comprehensive study of the effects of CO_2 purity of pipeline networks (Wetenhall et al., 2014) demonstrates that impurity levels below 2mole% do not affect the cost of the pipeline (except in the presence of hydrogen). In their study a

constant pressure loss gradient was used for the whole pipeline, but heat exchange with the environment (soil) was included. The cost function was based on the outside diameter of the pipeline.
Our study includes the compression, pipeline and booster stations and analyses the energy penalty and cost implications of two hypothetical impurity scenarios. Simultaneous heat transfer and pressure loss along the pipeline are included, using real, local physical properties and established correlations for frictional pressure loss and heat transfer coefficient.

2 Methodology

This study utilizes a methodology for integrated techno-economic assessment (Jakobsen et al., 2011; Jakobsen et al., 2014) on selected case studies for CO_2 transport with different impurity levels in the CO_2 feed stream. The boundary condition for this study is the scrubbed CO_2 stream that enters the compression and drying stages ahead of the pipeline transport – the "conditioning for transport". The feed stream is humid CO_2 that may contain residual components from the source stream or the capture process. The effects of impurities will affect the vapour/liquid separation efficiency ahead of each compression stage, the compression power, the cooling surfaces required and the cooling water energy consumption, and it will affect the state (temperature and pressure) of the gas at the point where the actual pipeline transport begins. This study estimates the energy and the material and labour costs for the conditioning part and for the transport part, in order to determine the optimal pipeline diameter, the required number of booster stations and to evaluate the economic penalty imposed by transporting impure CO_2 over long distances. This cost must be evaluated against the costs of capture and capture ratio. When a detailed analysis is performed that will also become case-specific.

2.1 Case studies

The feed gas for the case study is humid CO_2 under atmospheric conditions that includes impurities from two possible capture processes – but before the compression and water removal processes that precede transport by pipeline. The flow rate is 500 kg/s (13.1 MTPA) of CO_2 over a distance of 500 km. This is the identical to the case used by Roussanaly et al. (2013a). The conditioned gas is dried from about 5-600 ppm to 350 ppm before transport. The feed stream specifications are related to: a) capture from oxy-fuel combustion ("OXY"-feed) and b) natural gas sweetening process ("GAS"-feed). The base case is a feed stream with pure CO_2 saturated with water vapour (93% CO_2 and 7% H_2O) under atmospheric conditions, and the impurities that are added for the "GAS" and "OXY" cases are listed below in Table 1.

Table 1: Feed compositions used in this study

	CO_2 (mole %)	H_2O (mole %)	N_2 (mole %)	O_2 (mole %)	CH_4 (mole %)
"BASE"	93.0	7.0	-	-	-
"GAS"	83.0	7.0	1.0	-	9.0
"OXY"	88.0	7.0	3.0	2.0	-

The transport pressure is set at 150 bar and four different pipeline diameters (18", 20", 24" and 28") are studied with respect to the number of booster stations required and the maximum pressure loss. The various thermo-physical properties are calculated locally along the pipeline and the total energy consumption is found by integrating the local pressure loss and specific power along the pipeline. Heat transfer between the gas and its ambient is also included. The purpose of the case studies is to demonstrate the thermodynamic effects on hydraulic resistance in the pipeline when the evolution of local temperature and pressure are taken into account.

2.2 Technical modelling

It is therefore important to identify the effects of impurities on all thermo-physical properties in order to avoid operation with in a particularly unfortunate range of pressures and temperatures. It is also necessary to include the how the properties of the fluid change with temperature and pressure when CO_2 is transported over long distances. Variations in density are for example illustrated in Figure 1. The state-of-the-art review by (Knoope et al., 2013), showed that models used to predict the costs of CO_2

pipeline transport in many previous studies use constant values for the fluid density, either as pure CO_2 or for a given mixture in a single state point. Other comprehensive studies (Wetenhall et al., 2014) appear to have used a constant pressure-drop gradient in calculations of the pressure loss and the pumping power required over the length of the pipeline. If additional booster stations are required due to high hydraulic resistance in the pipeline, the cooling of the gas after recompression is taken into account. Our analysis uses the cooling capacity required for adiabatic recompression in its calculations. A failure to cool the recompressed gas could lead to an excessively high temperature after the booster station. Especially for small pipeline diameters, where the heat transfer surface is moderate, the temperature will rise, leading to vapour flow and excessive frictional pressure loss over long distances. Even if flow internal mass flux and inside heat transfer coefficient will increase, the heat transfer resistance is totally dominated by the external heat transfer through the soil and surface.

2.2.1 Thermo-physical models

One of the most important thermo-physical properties related to pipeline transport of CO_2 is fluid density. The effect of impurities is illustrated in Figure 1. In the dense phase the fluid behaves like a liquid at low temperatures but more gas-like at higher temperatures. At moderate pressures, illustrated here for 80 bar, this shift is quite sharp, and depending on the composition of the fluid it will occur at different temperatures or pressure ranges. Locally, at about 30 °C, the difference in density may be as high as 50%. At higher pressures, the shift between liquid and gas-like properties is more gradual.

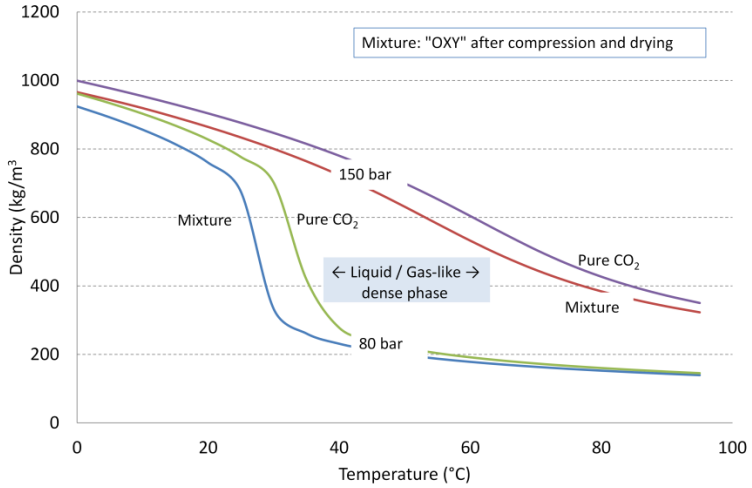

Figure 1: Effects of impurities on fluid density under pipeline transport conditions

When the CO_2 is transported over a long distance, the inlet pressure will typically be 150 bar, while the maximum pressure loss before reboosting can typically be 50-60 bar. Furthermore, depending on the level concentration of residual components, the temperature after the last compression or pumping stage at 150 bar will be in the range of 35-55 °C for the mixtures that have been investigated. This means that the pipeline inlet flow will be in a gas-like state unless additional cooling is performed. For a buried on-shore pipeline, heat transfer between the fluid in the pipe and the ambient is quite low and it will need to be transported for many miles before it reaches the more favourable liquid-like state. This will be illustrated in the results section.

The Peng-Robinson equation of state (Peng and Robinson, 1976) is used to calculate the thermodynamic properties and vapour-liquid equilibrium, while corresponding state methods (Huber and Ely, 1992; Huber et al., 1992) are used for transport properties such as viscosity and thermal conductivity.

2.2.2 Compression, cooling and separation

In this analysis the compression of the captured CO_2 from low pressure ambient conditions to transport pipeline conditions is included in the analysis. During compression the remaining moisture in the flue gas is separated and condenses at each compression stage. The feed enters the first stage of compression at 1 atm and 25 °C, when it still contains 7 mole% of water. After compression, the fluid is cooled to 25

°C. This is within the two-phase region for the CO_2-H_2O mixture, and the water is separated out and the vapour is compressed to the next pressure level. The pressure levels at the various stages of this conditioning process are 3.3, 9.5, 28.0 and 85 bar. After the last vapour liquid separation, the water content is around 550-650 ppm. The limit for transport is set at 350 ppm based on the IMPACTS recommendations (Brunsvold et al.), and the remaining water is assumed to be removed in a dryer unit that is not modelled in detail here. The whole conditioning process is illustrated in the pressure-enthalpy diagram in Figure 2.The green dew lines represent the phase boundary for $CO_2$with 8, 6, 4 and 2 mole % H_2O.

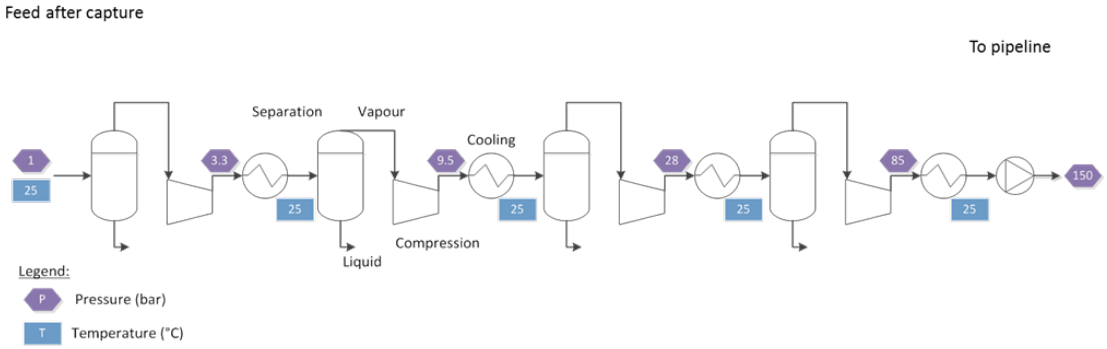

a) Separation – compression and cooling process

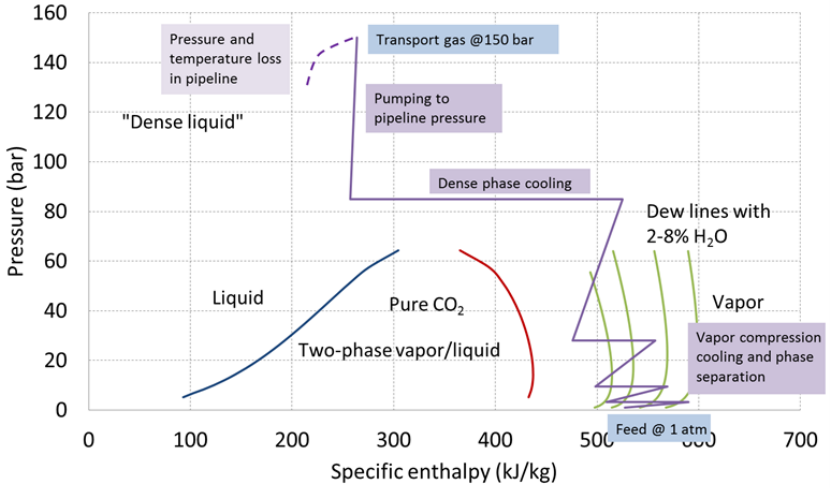

b) The compression route in the pressure-enthalpy diagram

Figure 2: Compression and conditioning before transport

The power consumption for the conditioning part is calculated as a sum of the compression and pumping power for all compression stages. An isentropic efficiency (η_{is}) of 85% is used for all stages, *i*, and the theoretical power consumption is calculated as according to eq. (1)

$$w_{teo,i} = \dot{m}_i \frac{\Delta h_{is,i}}{\eta_{is}} \quad (1)$$

$\Delta h_{is,i}$ is the increase in specific work between the compressor inlet and an isentropic outlet at discharge pressure.

2.2.3 Pipeline transport

The characteristics and modelling assumptions that are used for the pipeline are:

- It is onshore, uninsulated and the location is Europe
- The material is steel with a thermal conductivity of 55 W/(m·K)
- The surface roughness of the pipe wall is 47.5 µm

- The centre of the pipeline is 1.0 m below the surface
- The soil thermal conductivity is 2.4 (W/m·K)
- The average ambient temperature is assumed to be 15 °C, with a convective/radiative heat transfer coefficient of 5 W/(m²·K)
- Minimum permitted pressure in the pipeline is 90 bar
- The pipeline location classification is set to Class 4, with a utilization factor of 0.55
- The calculations are based on steady-state operation

The pressure loss results are quite sensitive to the thermal conductivity of the soil, so they will need to be estimated for specific sites in future case studies. Several typical values are found in the literature, e.g.1.2 W/(m·K) (Witkowski et al., 2013) and 2.6 W/(m·K) (Wetenhall et al., 2014)

2.2.3.1 Pressure drop and heat transfer models

The inside heat transfer coefficient and frictional pressure losses are calculated from the flow rate, composition and the local temperature and pressure. In the analysis the total pressure loss and estimated compression power required are calculated for the different pipeline diameters. When the minimum pressure of 90 bar is reached, a booster station will be required in order to re-compress the fluid to the transport pressure of 150 bar. The booster compression in this analysis is calculated to be done adiabatically, meaning that the heat added by the compression work is removed by cooling. If the added heat from compression is not removed, the temperature may increase at each booster station and with small pipeline diameters, the heat transfer surface will not be sufficient to remove the added heat during transportation. This will bring the fluid to a more gaseous state, with the consequence of excessive frictional pressure loss (and further temperature rise).

The rather simple calculation model used for compare the effects of the impurities includes the following sub-models:

- Frictional pressure loss
- Heat transfer between the pipeline gas and pipeline wall
- Heat transfer between the pipeline and the surface
- Numerical integration of pressure loss and heat transfer
- Thermodynamic and transport properties that are dependent on the local temperature and pressure in the pipeline

The frictional pressure loss in the model is calculated using the hydraulic model from (Selander, 1978) for wall friction.

Friction factor, *f*, from Selander

$$1/\sqrt{f} = 1.9 \cdot \log_{10}\left(\frac{10}{\mathrm{Re}} + \frac{0.2k}{D}\right) \quad (2)$$

where *k* is the surface roughness of the pipeline, Re is the Reynolds number and *D* is the hydraulic diameter (pipeline internal diameter in this case).

The pressure-loss gradient is related to the wall friction factor as follows:

$$\frac{dp}{dl} = -f\frac{\dot{M}^2}{2 \cdot \rho \cdot D} \quad (3)$$

where $\dot{M}$ is the mass flux (kg/m²s), ρ is the fluid density (kg/m³) and *D* is the pipeline's internal diameter (m).

The theoretical power consumption gradient (W/m) relates to the pressure drop as follows:

$$\frac{dw}{dl} = \frac{\dot{M} \cdot \pi \cdot D^2}{4 \cdot \rho} \cdot \frac{dp}{dl} \tag{4}$$

and is used to find the total pumping power required to overcome the friction resistance in the pipeline.

For the heat transfer calculations, an overall heat transfer coefficient is estimated based on the convective heat transfer between the fluid and the pipe wall and the conductive heat transfer through the pipe wall and the soil and convective/radiative heat transfer between the soil surface and the ambient The concept of using shape-factors for the ground heat transfer was employed in this analysis. The overall heat transfer coefficient, *U*, is calculated as shown in Eq.(5)

$$\frac{1}{U} = \frac{1}{\alpha_i} \cdot \frac{D_o}{D_i} + \frac{D_o}{2\lambda_p} \cdot \ln\left(\frac{D_o}{D_i}\right) + \frac{1}{S \cdot \lambda_s} + \frac{1}{\alpha_\infty} \tag{5}$$

where α_i and α_∞ are the inside and ambient heat transfer coefficients (W/m²K), D_i and D_o the inner and outer pipeline diameters and λ_p and λ_s are the thermal conductivities of the pipe and the soil respectively (W/m K). *S* is the shape factor for a buried horizontal cylinder at a depth, *z*, as shown in Figure 3 and Eq. (6). T_0 and T_1 is the ambient and pipeline outside wall temperatures. The diameter *D* is the pipeline's external diameter.

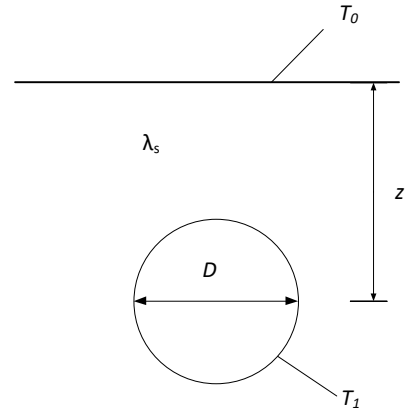

$$S = \frac{2\pi}{\cosh^{-1}\left(\frac{2z}{D}\right)} \tag{6}$$

Figure 3: Shape factor for buried cylinder

For the inside heat transfer coefficient, the simple Dittus-Boelter correlation is used as given in Eq.**(**7**)**

$$\mathrm{Nu} = \frac{\alpha_i D_i}{\lambda} = 0.023\ \mathrm{Re}^{0.8}\mathrm{Pr}^{0.3} \tag{7}$$

Here λ is the thermal conductivity of the fluid and the Pr-number is defined as:

$$\mathrm{Pr} = \frac{\mu C_p}{\lambda} \tag{8}$$

C_p and λ is the specific heat capacity (kJ/kg K) and dynamic viscosity (Pa s)

The heat flux is found as the relation: $\dot{q} = \left(\frac{\Delta T}{R}\right)_{\mathrm{tot}}$ where ΔT is the total temperature difference between the ambient and transported fluid, and *R* is the total heat transfer resistance: $R = {}^{1}/_{U}$.

The specific enthalpy gradient is calculated from the heat transfer as:

$$\frac{dh}{dl} = \frac{4 \cdot D_i \Delta T_{\text{tot}}}{\dot{M} R_{\text{tot}}} \tag{9}$$

For the numerical integration of the heat transfer rate and pressure drop along the pipeline, a standard 4th order Runge-Kutta scheme was employed. The three differentials are *dp/dl*, *dh/dl* and *dw/dl* for the pressure, specific enthalpy and specific work, respectively. The pressure and specific enthalpy are integrated from the inlet of the pipe line to the end of the pipeline. A booster station can be positioned along the pipeline either at fixed positions or according to a maximum permissible pressure drop. In the simulations, a 60 bar pressure loss, or a minimum pressure of 90 bar are used. The total pressure drop at any position L in the pipeline is calculated as $\Delta p = P_o - P_L$, where P_0 is the pressure at the pipe inlet. Likewise, the transferred heat is calculated as $\Delta Q = \dot{m}(h_0 - h_L)$ where h_0 is the specific enthalpy at the pipe inlet. Here, $\dot{m}$ is the mass flow rate in kg/s.

As can be seen, the calculations are performed in a pressure-specific enthalpy space. That means that all the local thermodynamic properties and transport properties must be retrieved from the local values of *p* and *h*. This is done by performing a thermodynamic *pressure-enthalpy flash* using the selected equation of state. With the calculated temperature, the fluid phase and all the other properties, such as density, dynamic viscosity, thermal conductivity and specific heat capacity can be calculated directly and be used in the expressions to get *dh/dl* and *dp/dl*.

If the pipeline gas is in a two-phase state, the local vapour fraction and fluid composition in each phase are calculated. With the temperature, pressure and local vapour and liquid composition, the other properties like density, dynamic viscosity, thermal conductivity and specific heat capacity can be directly calculated for each phase. For the underlying expressions for *dh/dl* and *dp/dl*, Eq. (2), (3) and (7), the same expressions as for single phase state are used, but homogeneous two-phase density, viscosity, thermal conductivity and specific heat capacity are used, calculated from the phase-specific values and the vapour fraction *x*. This is a simplification, compared to applying specialized two-phase expression for heat transfer and pressure drop, but is justified in this analysis, in which the quantitative effects of impurities are investigated and the two-phase region is only approached when the flow rate is too high or the pipeline diameter too small.

The homogenous two-phase properties are calculated according to the equations below.

Vapour fraction from molar to mass basis:

$$x = \frac{w \cdot M_{\text{vap}}}{M_{\text{tot}}} \tag{10}$$

Specific heat capacity:

$$c_p = x c_{p,\text{vap}} + (1 - x) c_{p,\text{liq}} \tag{11}$$

Thermal conductivity:

$$\lambda = x \lambda_{\text{vap}} + (1 - x) \lambda_{\text{liq}} \tag{12}$$

Dynamic viscosity:

$$\frac{1}{\mu} = x \frac{1}{\mu_{\text{vap}}} + (1 - x) \frac{1}{\mu_{\text{liq}}} \tag{13}$$

Density:

$$\rho = \alpha \rho_{\text{vap}} + (1 - \alpha) \rho_{\text{liq}} \tag{14}$$

The void fraction, α, which is a volume- or area-based phase fraction in two-phase flow, can be calculated from an appropriate correlation, the simplest flow regime is homogeneous flow, with no slip between the vapour and liquid phases. To calculate the volumetric vapour fraction, the Rouhani-Axelsen (Rouhani and Axelsson, 1970) void fraction correlation in eq. **(**15) was used

$$\frac{x}{\rho_{\text{vap}}}\alpha = 1 + 0.12(1-x)\cdot\left(\frac{x}{\rho_{\text{vap}}} + \frac{1-x}{\rho_{\text{liq}}}\right) + \frac{1.18(1-x)\cdot\left[g\cdot\sigma\left(\rho_{\text{liq}} - \rho_{\text{vap}}\right)\right]^{0.25}}{\dot{M}\sqrt{\rho_{\text{liq}}}} \quad (15)$$

2.2.3.2 Material selection and pipeline wall thickness

This analysis investigates external pipeline diameters of 18", 20", 24" and 28". The minimum required wall thickness is calculated according to the recommendations outlined by DNV (Det Norske Veritas, 2010), where the minimum wall thicknesses to withstand internal pressure t_{minDP}, and fracture propagation, t_{minDF}, need to be calculated. The larger of the two wall thicknesses should then be selected for each pipeline diameter. To calculate these t_{minDP} equation (16) is used

$$t_{\text{minDP}} = \frac{P_D \cdot R_{\text{o}}}{\sigma_0}\cdot\frac{1}{f} \quad (16)$$

where P_d is the design pressure, R_o is the outside pipeline radius, and σ_0 is the yield strength.
The utilization factor f is determined by the location classification for the pipeline. This analysis utilised class 4, with a value of 0.55 for f. To calculate $t_{\text{minDF,}}$ the value of the cricondenbar (maximum pressure on the phase envelope) for the CO_2 mixtures is compared to the estimated arrest pressure for the pipeline. The reason for using the cricondenbar as a design pressure can be illustrated from the following argument:

If a pipeline is accidently damaged and a crack appears, whether the crack will arrest or be propagated will depend on the material properties and of the initial state of the fluid and its thermodynamic properties. This is illustrated schematically in the figure inserted on the left of Figure 4. To the right, a crack occurs at time ① and the pressure falls rapidly until a "plateau" is reached at time ②. After a while, ③, the pressure continues to fall until ambient pressure is reached. The plateau pressure is closely related to the saturation pressure for the fluid mixture. During the initial depressurization, the expansion to a lower pressure is isentropic, following constant specific entropy from the initial to the saturation pressure. Figure 4 also illustrates the principle of isentropic expansion in the pressure-temperature diagram. The slope of the constant specific entropy line depends on the thermodynamic situation, and its accuracy is based on caloric properties such as specific heat capacity, and the equation of state. It is also easy to see how expansion from an equal temperature and pressure can lead to a significantly higher saturation pressure for a CO_2 mixture than for pure CO_2. In the illustration, this has increased from 55.4 bar for pure CO_2 to 78.3 bar for the "GAS" mixture.

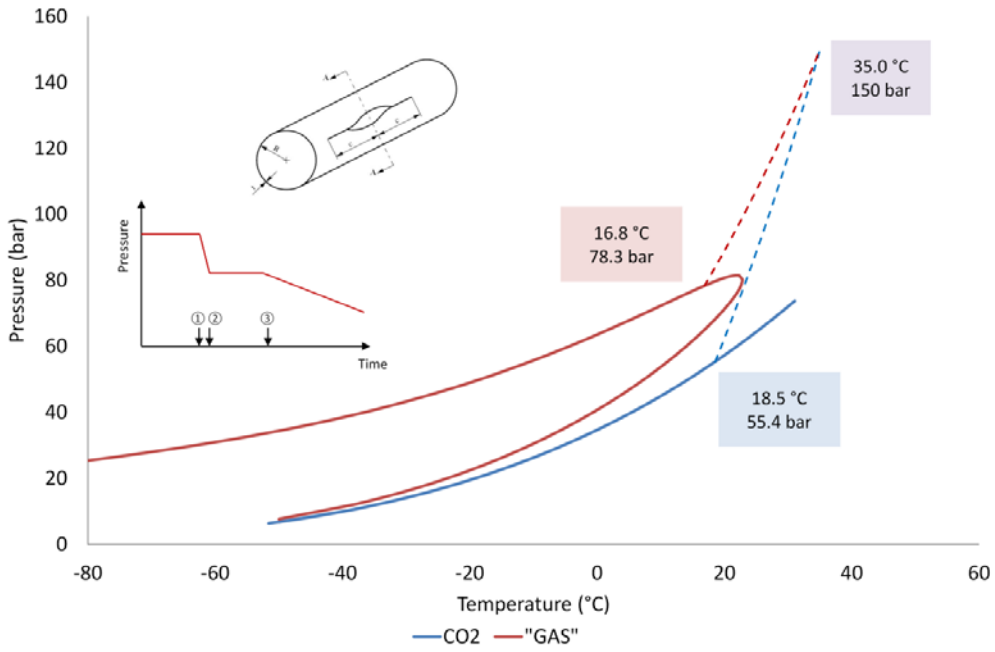

Figure 4: Isentropic expansion from ① to ② until the phase boundary is reached for pure CO_2 and for the "GAS"-mixture

When the minimum wall thickness needed to avoid fracture propagation is being determined, the maximum saturation pressure for the fluid mixture needs to be located. In Figure 5, the expected operational envelope in terms of temperature and pressure is shown in a pressure-entropy diagram. An isentropic expansion in such a diagram will take the form of a vertical line from the initial condition to the saturation line. The maximum and minimum pressures in the pipeline are shown as horizontal lines and the constant temperature lines for the maximum and minimum temperatures are calculated and appear as dashed lines.

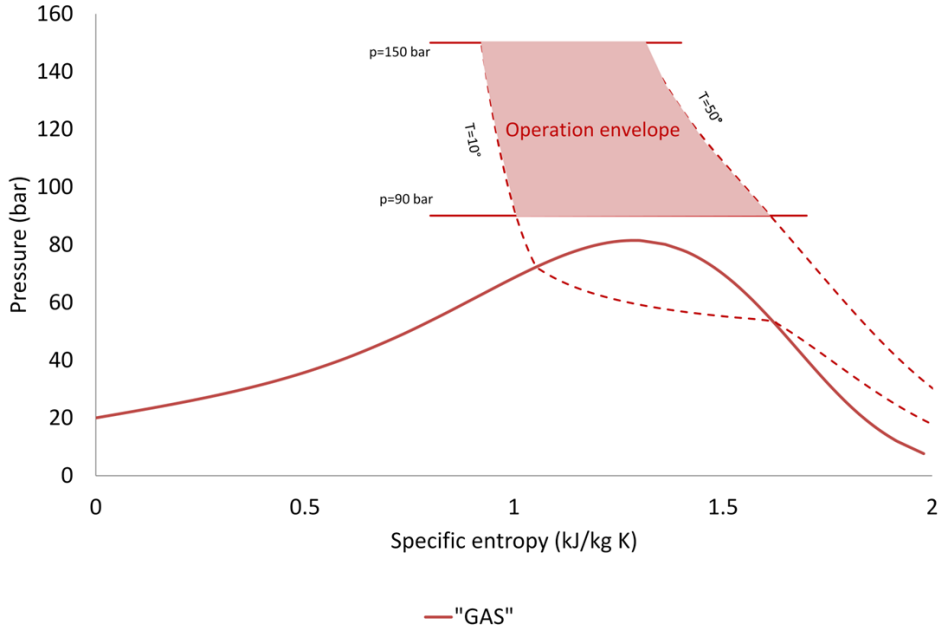

Figure 5: Phase envelope for the "GAS" mixture including the possible operational envelope for the pipeline study

The minimum pressure in the pipeline needs to be above the two-phase region, which means above the cricondenbar (also referred to as the maxcondenbar). In the current analysis, this is set at 90 bar, which

also means that recompression will take place if the pressure falls below this. This in turn means that during transport, the fluid may undergo several cycles of cooling, recompression and heating. For this reason, the calculated arrest pressure for the pipeline needs to be above the cricondenbar when the required minimum wall thickness, t_{minDF} is being calculated. This analysis employs, the standard Battelle Two-Curve Model (TCM) approach with the inclusion of an additional correction factor c_{cf}=1.2. The correction factor is included in order to take into account the fact that the TCM approach is believed to be non-conservative for use with CO_2-mixtures. (Jones et al., 2013) show that the deviation between predictions and the results of full scale experiments becomes smaller towards the top of the phase envelope The arrest pressure (p_a) as a function of pipeline radius (R_o), wall thickness (t) and material properties can be expressed as eq. (17) (Aursand et al., 2014)

$$p_a = \frac{2 \cdot t \cdot \tilde{\sigma}}{3.33 \cdot c_f \cdot \pi R_o} \cdot \cos^{-1}\left[e^{\left(\frac{\pi R_f E}{24\tilde{\sigma}^2\sqrt{R_o \cdot t}}\right)} \right] \qquad (17)$$

The material properties required for this analysis are the “fracture toughness” per fracture area, R_f , which is related to the Charpy V-notch energy (CVP), the yield strength, σ_0, the “material flow stress”, $\tilde{\sigma}$, and the elasticity, E. For X70 carbon steel the following material properties are used:

Table 2: Material properties for X70 carbon steel

	Data used for the steel quality (X70)
R_f	$5.06 \cdot 10^6$ J/m^2 (Based on CVP = 250 J)
E	$2.06 \cdot 10^6$ Pa
$\tilde{\sigma}$ (Flow stress: $\sigma_0 + 68$ MPa)	$498 \cdot 10^6$ Pa
σ_0	$430 \cdot 10^6$ Pa
c_f	1.2

2.3 Cost evaluation methodology

This study assumes costs of a "NOAK" (Nth Of A Kind) plant to be built at some time in the future, when the technology is mature. Such estimates reflect the expected benefits of technological learning, but they may not adequately take into account the greater costs that typically occur in the early stages of commercialisation (Metz et al., 2005).

Two investment cost estimation methods are used: a general method for the CO_2 conditioning and a more specific one for the CO_2 transport. Investment and operating costs are given in 2014 prices. Where necessary, the investment costs of the conditioning plant and the pipeline are updated according to the Chemical Engineering Plant Cost Index (CEPCI) (Chemical Engineering, 2015) while the utilities costs are corrected in accordance with an annual inflation index of 2% (Trading Economics, 2011).

2.3.1 Investment costs

A factor estimation method is used to estimate the investment costs of CO_2 conditioning processes and booster stations, where the estimated direct costs (including piping/valves, civil engineering works, instrumentation, electrical installations, insulation, painting, steel structures, erections and outside battery limits) are multiplied by an indirect cost factor (including yard improvement, service facilities, engineering/consultancy costs, building, miscellaneous, owner's costs and contingencies) to obtain the investment costs. Direct costs of the CO_2 conditioning process in suitable materials are estimated using Aspen Process Economic Analyzer® (AspenTech, 2010), based on results from the technical design, while cost of the CO_2 pumps, due to their specificity, is estimated based on literature (Roussanaly et al., 2013a). The total investment is then determined by multiplying the sum of direct costs by an indirect cost factor of 1.31 (Anantharaman et al., 2011).

For pipeline transport, the pipeline investment costs are assessed following the cost model proposed by Knoope et al. (Knoope et al., 2014). This cost model, adapted to onshore pipelines is based on the following set of equations:

$$I_{\text{pipeline}} = I_{\text{material}} + I_{\text{labor cost}} + I_{ROW} + I_{\text{Miscellaneous}}$$

$$I_{\text{material}} = \frac{\pi}{4} \cdot (D^2 - (D - 2t)^2) \cdot L \cdot \rho_{\text{steel}} \cdot C_{\text{steel}}$$

$$I_{\text{labor cost}} = C_{\text{labor}} \cdot D \cdot L$$

$$I_{ROW} = C_{ROW} \cdot L$$

$$I_{\text{Miscellaneous}} = 25\% \cdot (I_{ROW} + I_{\text{Miscellaneous}})$$

Where:
I_{pipeline} is the pipeline investment cost combining the costs associated with materials, labour, rights of way and miscellaneous costs.
I_{material} is the pipeline materials cost, based on its external diameter (D), thickness (t) and length (L), the steel density (ρ_{steel}) equal to 7900 kg/m^3, and the steel cost (C_{steel}) equal to 1.57 €$_{2014}$/kg.
$I_{\text{labor cost}}$ is the pipeline labour cost calculated on the basis of a unitary labour cost (C_{labor}) of 22.1 €$_{2014}$/in/m, combined with the pipeline external diameter and the pipeline length
I_{ROW} is the pipeline right of way (ROW) cost estimated on the basis of a unitary ROW (C_{ROW}) equal to 87.4 €$_{2014}$/m and combined with the pipeline length
$I_{\text{Miscellaneous}}$ includes other costs and margins and is estimated at 25% of total materials and investment costs.

The investments are assumed to be shared over three years, with a 40/30/30 annual allocation of project finance over the construction time (Anantharaman et al., 2011).

2.3.2 Maintenance and operating costs

The fixed operating costs depend on the investment costs, and cover maintenance, insurance, and labour. The annual fixed operating cost is set at 6% of total direct costs for the CO_2 conditioning and booster stations (Chauvel et al., 2003), while the annual pipeline fixed operating costs are assumed to represent 1.5% of the investment cost (Knoope et al., 2014).
The variable operating costs are a function of the amount of CO_2 transported, and cover consumption of utilities: electricity and cooling water. The annual variable operating costs are estimated using the consumptions of utilities given by the simulation results and utility costs shown in Table 3. As one of the main objectives of this study is to calculate the CO_2 conditioning and transport costs in order to quantify the impact of impurities, no CO_2 tax is taken into consideration.

Table 3: Utility costs

Utilities	Reference costs	Cost Units
Cooling water cooling (Fimbres Weihs and Wiley, 2012)	0.039	€/m^3
Electricity cost (Koring et al., 2013)	80	€/MWh

2.3.3 Key Performance Indicators for comparison of the options

In order to evaluate the cost impact of impurities, the CO_2 conditioning and transport cost [€/t$_{CO2,avoided}$], as defined below, is used as Key Performance Indicator. The CO_2 avoided transport cost approximates the average discounted CO_2 tax or quota over the duration of the project that would be required as income to match the net present value of additional capital and operating costs due to the CO_2 conditioning and transport infrastructure. The CO_2 conditioning and transport cost is calculated

assuming a real discount rate of 8%[1], 7,500 operating hours per year and an economic lifetime of 25 years (Anantharaman et al., 2011). The annual direct CO_2 emissions are defined as the amount of CO_2 generated from electricity consumption in the conditioning and transport processes. An electricity climate impact of 435 g_{CO2}/MWh is assumed for calculations (Covenant of Mayors, 2010).

$$\text{CO}_2 \text{ conditioning and transport cost} = \frac{\text{Annualized Investment} + \text{Annual OPEX}}{\text{Annual amount of CO}_2 \text{ transported} - \text{Annual direct CO}_2 \text{ emissions}}$$

3 Results and discussion

The impact of impurities on the technical and cost performances of CO_2 conditioning and transport are presented and discussed below. In addition to its influence on the design and cost of a pipeline, the impact of impurities on the performances of a pipeline infrastructure design for a case without impurities is also discussed.

3.1 Pipeline characteristics

When the calculation of the t_{minPD} and t_{minDF} using the methodology explained in section 2.2.3.2 are superimposed, a diagram such as shown in Figure 6 can be constructed for any given pipeline.

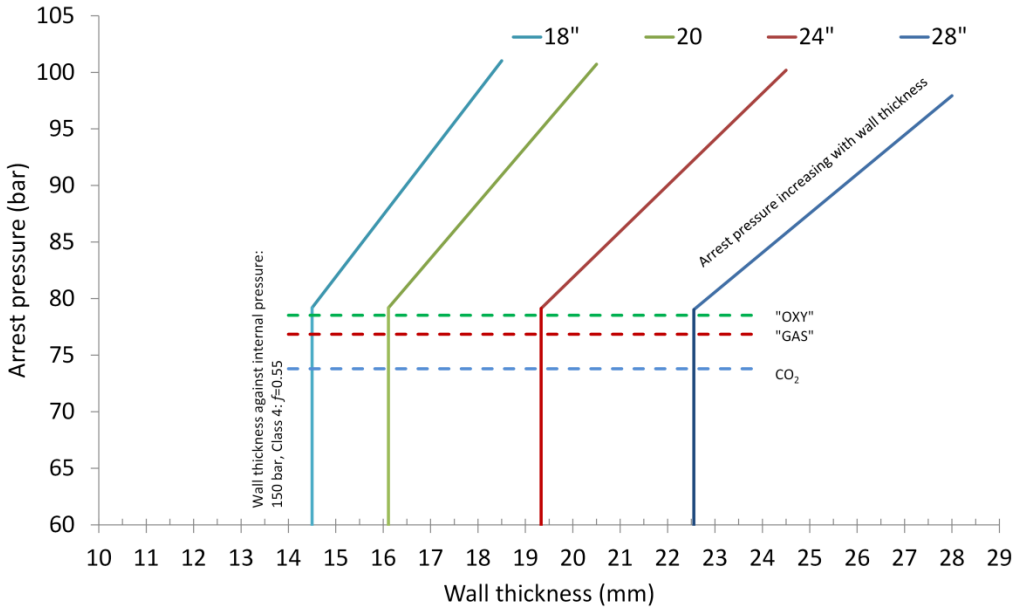

Figure 6: Minimum wall thickness required to withstand internal pressure and prevent fracture propagation for X70 carbon steel pipelines of different diameters

The vertical lines indicate the minimum wall thickness required for 150 bar internal pressure and a utilization factor of 0.55. The tilted lines show the calculated arrest pressure from eq. (17) for a range of wall thicknesses. The four set of curves represent the four pipeline diameters investigated in this analysis. The dashed horizontal lines are the calculated cricondenbar for the base and the two CO_2 mixtures "GAS" and "OXY". In this case, with the Class 4 pipeline location (according to ISO 13623) the minimum wall thickness against the internal pressure will be the larger of the two. For a given pipeline route the location class can range from 1 to 5 with a corresponding utilization factor that varies between 0.83 and 0.45. From the diagram shown in Figure 6, this impl that for a location class lower than 4, the minimum wall thickness needed to prevent fracture propagation will be the larger one for the mixtures investigated. For a mixture with a higher maximum saturation pressure than the "OXY" case, a thicker wall will also be necessary, for instance for a completely dry mixture or one containing traces of hydrogen.

[1] This real discount rate of 8% corresponds to a nominal discount rate around 10% if an inflation rate of 2% is considered.

Once the minimum required wall thickness has been found, 1.5 mm is added for corrosion protection plus 12.5% for manufacturing defects. The wall thickness is then rounded up to the nearest available dimension for the given pipeline diameter according to the API 5L standard (API, 2004) as listed in Table 2.

Table 4: Pipeline wall thicknesses used in the analysis

Pipeline diameter		18"	20"	24"	28"
Wall thickness		¾ "	13/16"	15/16"	1 1/8"
	(mm)	19.1	20.6	23.8	28.6
Inside diameter	(mm)	419.1	466.7	562.0	654.0

3.2 Impact of impurities on CO_2 transport design and cost

In this section, the impact of impurities on the design and cost of the CO_2 conditioning and transport is investigated for the three impurity cases considered. The design is assumed to take place knowing the impurity case which will be transported through the pipeline.

3.2.1 Impact on technical and energy performances

The energy consumption in kWh/tonnes CO_2 for the four compression stages plus the last pumping stage from 85 bar to the transport pressure of 150 bar is shown in Figure 7. In this analysis, with 5% combined N_2 and O_2 impurities, the energy consumption increased by approximately 5 kWh/tonne CO_2, while with 9% methane impurity plus 1% N_2, the compression energy required rose by approximately 10 kWh/tonne CO_2, from 67.35 to 77.48,compared to the base case with only CO_2 and H_2O. The energy requirements for cooling the fluid from the compressor discharge temperature to 25 °C are161, 159 and 165 kWh/tonne CO_2 for the base-, "OXY"- and "GAS"-case respectively.

In the separations prior to each compression stage, the liquid phase consists of more than 99% water, so virtually no CO_2 or any of the impurities will be present. For all cases the transported flow rate where the water has been removed has been reduced from 500 kg/s to about 485 kg/s for all cases.

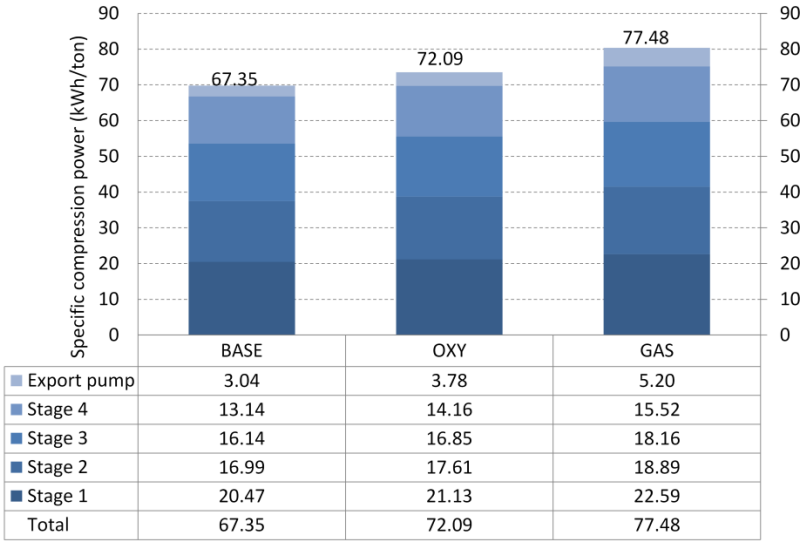

	BASE	OXY	GAS
Export pump	3.04	3.78	5.20
Stage 4	13.14	14.16	15.52
Stage 3	16.14	16.85	18.16
Stage 2	16.99	17.61	18.89
Stage 1	20.47	21.13	22.59
Total	67.35	72.09	77.48

Figure 7: Specific energy consumption for the compression and drying of the CO_2 feed stream

The specific energy consumption shown in Figure 8 is the compression power required to overcome the pipe friction.

For the pipeline transport, the number of required booster station will increase quite dramatically when choosing smaller diameter pipelines which will require substantially more energy not only for re-compression but also for cooling. This is included in the Figure 8b.

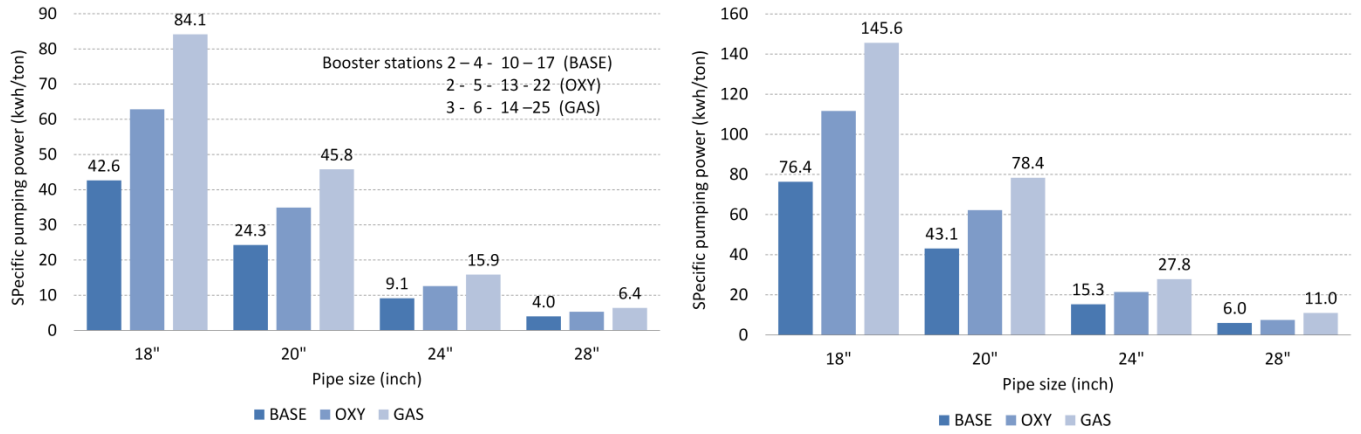

a) Transport b) Transport and booster stations

Figure 8: Specific energy consumption for pipeline transport of CO_2 with impurities

Some key numbers that explains the increased energy consumption and number of booster stations can are listed in Table 5. Here the mass flux (mass flow per cross sectional area), the compression power consumption and the number of booster stations that will be necessary for keeping a safe distance to the two-phase region for the three fluid streams that are considered. In this table, the last booster station will be the last compression to the injection pressure that is specified in this analysis to be 200 bar.

Table 5: Transport pipeline mass flux transport power consumption and number of booster stations

	Pipeline diameter:		18"	20"	24"	28"
"BASE"	Mass flux	(kg/m²s)	3363	2723	1891	1389
	Transport power consumption	(MW)	59.6	34.0	12.8	5.6
	Number of booster stations	(-)	17	10	4	2
"GAS"	Mass flux	(kg/m²s)	3510	2830	1952	1427
	Transport power consumption	(MW)	117.3	68.0	22.1	8.9
	Number of booster stations	(-)	25	14	6	3
"OXY"	Mass flux	(kg/m²s)	3515	2834	1955	1429
	Transport power consumption	(MW)	87.8	48.8	17.6	7.4
	Number of booster stations	(-)	22	13	5	2

As seen from the numbers in Table 5 there is no direct link between the mass-flux and the pressure loss or power consumption. The difference in composition between the mixtures will result in different temperature and density profiles and thus also Re-numbers and friction factors, so therefore it is necessary to perform specific analysis for each case. In the next part, the power and energy consumptions are used for operating costs for the different pipelines.

3.2.2 Impact on costs and optimal design

The results of the cost assessment of the conditioning and transport processes are presented in **Figure 9** for the three impurity cases ("BASE", "OXY" and "GAS") and the four pipeline diameters (18", 20", 24" and 28") considered.

The evaluation of conditioning costs shows that the presence of impurities in the CO_2 stream leads to a higher conditioning cost. Indeed, the conditioning investment and operating costs are directly linked to the conditioning power requirement and, as illustrated in section 3.1.1, the presence of impurities leads to a higher conditioning power demand. As a result, the specific CO_2 conditioning costs are 10 and 22% higher in the "OXY" and "GAS" cases respectively than in the "BASE" case.

With regard to CO_2 transport costs, the evaluation shows that, while the costs are different for each of the impurity cases, in each case a cost-optimal pipeline diameter exists, due to the trade-off between the pipeline investment cost and the electricity pumping cost (McCoy and Rubin, 2008; Roussanaly et al., 2014; Roussanaly et al., 2013b). For each of the three impurity cases considered, the cost evaluation

highlights that a 24" diameter pipeline is the most cost-efficient option. However, it is important to note that this result is specific to the transport system considered in this paper and that in principle, different impurity cases can lead to different cost-optimal diameters especially for low pipeline diameters. Moreover, even if the cost-optimal diameter is the same in each case, the specific transport cost for the cost-optimal diameter depends on the impurity case. Indeed, the specific transport costs are respectively 15 and 22% higher in the "OXY" and "GAS" cases than in the "BASE" case. For the cost-optimal diameter, this increase is mainly due to the higher costs of investment and maintenance, which are linked to the greater pipeline thicknesses and the larger number of pumping stations required in the cases with impurities. In addition, it is also important to note that smaller diameters can be expected to be even less favourable in cases with impurities, due to the impact of these on the pipeline pressure drops.

This therefore results in a significant increase in the conditioning and transport costs when CO_2 contains impurities. Indeed, in the "OXY" and "GAS" cases, the specific conditioning and transport costs are 13 and 22% higher respectively than in the "BASE" case for the cost-optimal pipeline diameter. In absolute values, these represent direct increases for specific conditioning and transport of 2.3 and 3.8 €/$t_{CO2,avoided}$ respectively.

Finally, while the costs discussed here considered only the impact of impurities on the conditioning and transport costs, impurities can also be expected to have a significant impact on the technical and economic performances of the whole CCS chain shown from the key results from the IMPACTS project (Brunsvold et al.)

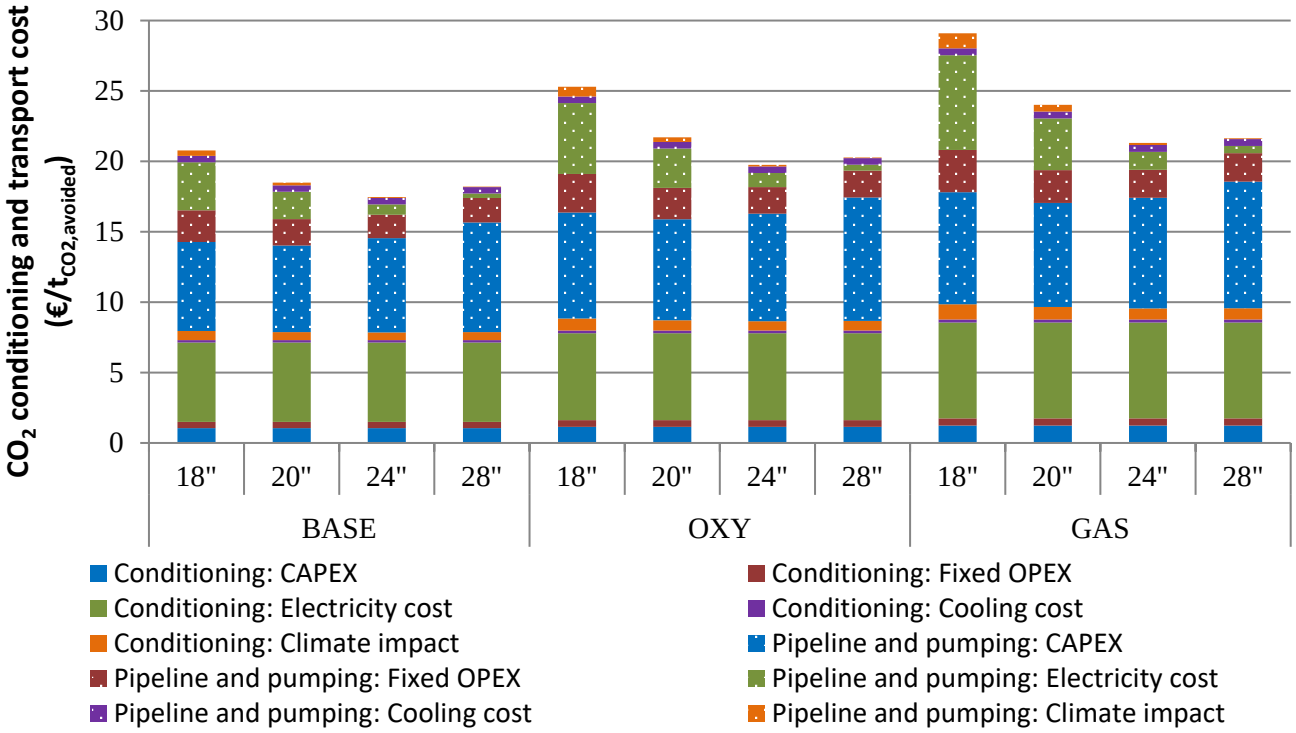

Figure 9: Specific CO_2 conditioning and transport cost of the "BASE", "OXY" and "GAS" cases for pipeline diameters from 18" to 28"

3.3 Effect of impurities on a designed pipeline

In this section, the impact of impurities on the operation and cost of CO_2 conditioning and transport is investigated for the three CO_2 cases considered for an existing pipeline infrastructure. The design is here assumed to have been done without considering the importance of potential impurities (i.e. is designed as for the "BASE" case) and the pipeline diameter is set to 24" according to the results presented in section 3.1.2. However to ensure safe transport, it is still assumed that the pipeline thickness has been selected for the most constraining case (i.e. the "GAS" case).

3.3.1 Impact on the technical and energy performances

This section evaluates the effects of impurities for a 24" diameter pipeline with four booster stations. With the installed compression from the base case where the feed of humid CO_2 is 500 kg/s, the feed flow rate for the GAS- and OXY-feeds are reduced to 432 and 465 kg/s respectively. The power consumption is ~17.6 MW for each of the cases. Once the water has been removed, the flow rates for the three cases are: 485.2 kg/s (BASE), 418.4 kg/s (GAS) and 451.0 kg/s (OXY).

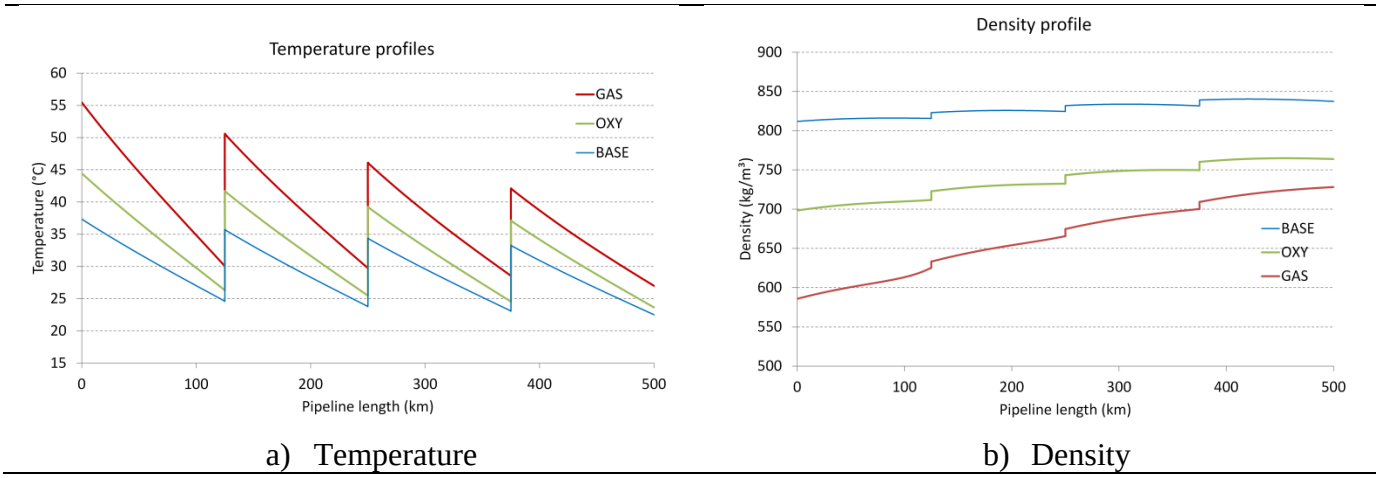

a) Temperature b) Density

Figure 10: Temperature and density profiles along a 24" pipeline with four booster stations

Figure 10 shows how impurities affect the temperature and density profiles along the pipeline. After conditioning, the temperature of the GAS-mixture enters the pipeline at a temperature of 55 °C, compared to the base case, where the temperature is 37.5 °C. The higher temperature of the CO_2 – stream with impurities the lower (more gaseous) will be the density and the higher the flow velocity and frictional pressure loss. This relates to Figure 1, where the impact of impurities shifts the temperature range within which the fluid changes from a dense-phase liquid to a dense-phase vapour. Because of the reduced flow rates of the impure CO_2 streams, the pressure profiles along the pipeline will be nearly identical in all three cases. This illustration shows that it could be advantageous to cool the CO_2 stream sufficiently before transport and after each re-compression stage to ensure a liquid-like dense phase state throughout the pipeline.

3.3.2 Impact on cost performances

As it is important to also understand the cost impact of transporting CO_2 with impurities via a pipeline that has been designed for a system without or with only a small amount of impurities, the results of the cost assessment of the conditioning and transport process are presented in **Figure 11** for the three impurity cases, in a 24" pipeline with four pumping stations.

Since in the "OXY" and "GAS" cases less CO_2 can be transported through the pipeline, four penalty-cost scenarios for these CO_2 emissions not transported are considered: 0, 10, 20 and 30 €/$t_{CO2\ not\ transported}$. This penalty cost can represent, for example, the costs associated with conditioning and transport of this CO_2 through a different pipeline or with releasing this CO_2 to the atmosphere and not fully using the installed CO_2 capture and storage capacity[2].

The cost evaluations presented in **Figure 11** show that a pipeline designed for a CO_2 stream without impurities and operated for a CO_2 stream with impurities can lead to significantly higher specific transport and conditioning costs. Indeed, if the pipeline is operated under "OXY" impurity case conditions, the specific conditioning and transport cost is between 8 and 22% higher than when the pipeline is operated for the "BASE" case, depending on the penalty cost scenario considered. Under the "GAS" impurity case, this increase is even greater and is between 18 and 46% higher than under the "BASE" impurity case.

[2] Even if the consumption of utilities can be reduced if the capture system is not fully used, investments and maintenance costs cannot be avoided, and these must be allocated to the transport limitations caused by the presence of impurities.

If the penalty cost for the CO_2 not transported is assumed to be 0 or 10€/$t_{CO2\ not\ transported}$, the specific conditioning and transport costs of the "OXY" and "GAS" cases are 8 to 13% and 18 to 27% respectively more expensive than in the "BASE" case. These numbers are rather similar to those mentioned in section 3.1.2, as here the pipeline is operated at its maximum capacity in each case and that the emission penalty cost remains rather small. However this scenario is representative of a CCS chain with very limited capture and investments and operating under low CO_2 emission penalty cost, and is therefore rather unlikely.

In the 20 and 30 €/$t_{CO2\ not\ transported}$ penalty cost scenarios, the specific cost of the "OXY" and "GAS" cases are 18 to 22% and 37 to 46% more expensive than in the "BASE" case. These numbers are even higher than those presented in section 3.1.2 due to the lesser amount of CO_2 transported and the important penalty associated with the CO_2 not transported. It is important to note than these two scenarios appear to be more realistic than the first two. Indeed, if the CO_2 emissions which could not have been transported in the infrastructure described here can be conditioned and transported through another pipeline infrastructure, the penalty cost can be expected to be in the range of the specific and conditioning and transport costs obtained in section 3.1.2 (around 20€/t). Moreover, if the CO_2 which could not be transported is released to the atmosphere, the penalty cost can be expected to be even higher than 20 €/t as it needs to take into account the costs associated with releasing this CO_2 to the atmosphere (CO_2 tax or quota) and the cost associated with not fully using the installed CO_2 capture and storage capacity.

In conclusion, large additional specific conditioning and transport cost can be expected in situations in which pipelines are operating with levels of impurities higher than the level for which they have been designed. This could make the inclusion of further steps to remove impurities even more attractive in such cases.

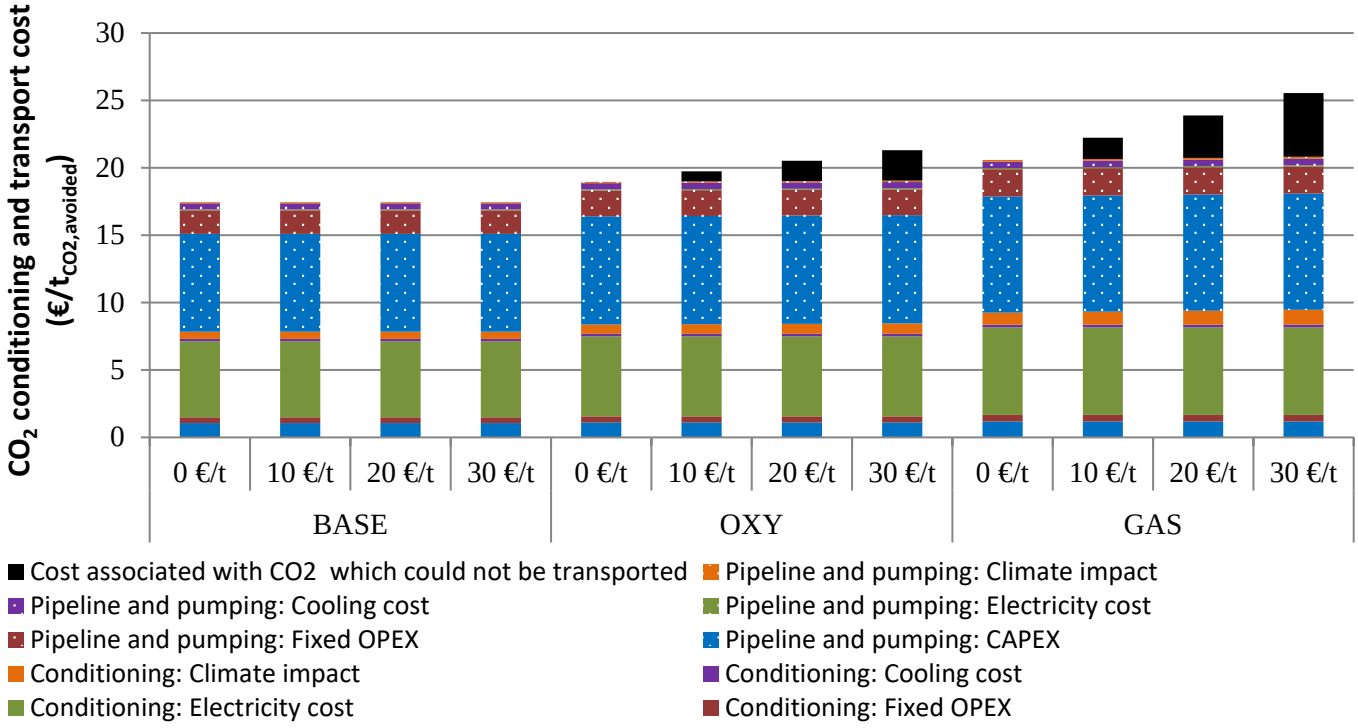

Figure 11: Specific CO_2 conditioning and transport costs of the "BASE", "OXY" and "GAS" cases for a 24" pipeline system designed for the "BASE" case with penalty cost ranging from 0 to 30 €/$t_{CO2\ not\ transported}$

4 Conclusions

This study analyses the effect of transporting 13.1 MTPA CO_2 with impurities over a distance of 500 km on the operating and investment costs. In the cases study, two different impurity levels coming as a result of gas sweetening (GAS) and from capture from oxy-fuel combustion (OXY). The analysis includes the cost for the conditioning and the compression of the CO_2 stream after capture from atmospheric conditions to transport conditions in the dense phase. In the calculation of the operating

cost, in terms of compression power and cooling requirements, the effect of the impurities are taken into account by using real thermo-physical properties depending of local fluid temperature and pressure and including heat transfer with the ambient. The analysis investigates the total cost of choosing different pipeline diameters for transporting CO_2. The technical analysis shows that the number of required booster stations increases from 2 to 17 between 28" and 18" pipeline and from 3 to 25 in the worst case. In the second technical comparison, the feed flow rate for the CO_2 mixtures has been reduced so that the installed compression power will be equal for all cases. In this analysis a 24" pipeline with 4 booster stations was used.

The techno-economic assessments show a significant impact of the impurity cases considered on the CO_2 conditioning and transport design and cost. Indeed, in the Oxy-feed and Gas-feed cases, the specific conditioning and transport costs are respectively 13 and 22% higher than in the Base-feed case for the cost-optimal diameter. In absolute value, this represents a direct increase of the specific conditioning and transport cost of 2.3 and 3.8 €/$t_{CO2,avoided}$. Even if the cost evaluation leads to the same cost optimal diameter for the three impurity cases considered, it is important to note that this result is specific to the transport system considered in this paper and that in principle different impurity cases can lead to different cost-optimal diameters especially for low pipeline diameters.

The impact of impurities on an existing pipeline infrastructure design not taking into account these potential impurities show an even stronger cost impact. Indeed, the cost evaluations shows that the specific cost of the Oxy-feed and Gas-feed cases can be expected to be respectively at least around 20 and 40% more expensive than in the Base-feed case due to the lower amounts of CO_2 transported and the important cost-penalty associated with the CO_2 emissions not transported.

Finally, while the cost presented here considered only the impact of impurities on the conditioning and transport cost, impurities can also be expected to have a significant impact on the technical and economic performances of the whole CCS chain (Brunsvold et al.)This therefore highlights the importance of evaluating, on a case-to-case basis, the trade-offs between impact of impurities on the CCS cost and cost of impurities removal in order to provide recommendations on cost-optimal level of impurities along the chain.

Acknowledgements

This study was financially supported by the European Community's Seventh Framework Programme (FP7-ENERGY-20121-1-2STAGE) under grant agreement no. 308809 (The IMPACTS project). The authors gratefully acknowledge the project partners and the following funding partners for their contributions: Statoil Petroleum AS, Lundin Norway AS, Gas Natural Fenosa, MAN Diesel & Turbo SE and Vattenfall AB.

REFERENCES

Anantharaman, R., Bolland, O., Booth, N., Dorst, E.V., Ekstrom, C., Franco, F., Macchi, E., Manzolini, G., Nikolic, D., Pfeffer, A., Prins, M., Rezvani, S., Robinson, L., 2011. D1.4.3 European best prectice guidelines for assessment of CO2 capture technologies. DECARBit Project.

AspenTech, 2010. Aspen Icarus Reference Guide, Burlington

Aursand, E., Dørum, C., Hammer, M., Morin, A., Munkejord, S.T., Nordhagen, H.O., 2014. CO2 Pipeline Integrity: Comparison of a Coupled Fluid-structure Model and Uncoupled Two-curve Methods. Energy Procedia 51, 382-391.

Brunsvold, A., Jakobsen, J.P., Mazzetti, M.J., Hammer, M., Eickhoff, C., Neele, F., Key Findings and Recommendations from the IMPACTS Project, Int Journal of Greenhouse Gas Control.

Chauvel, A., Fournier, G., Raimbault, C., 2003. Manual of Process Economic Evaluation. Editions Technip.

Chemical Engineering, 2015. Economic Indicators: Chemical Engineering Plant Cost Index (CEPCI).

Climate change, 2014. Mitigation of climate change, IPCC Fifth Assessment report. Available from http://ipcc.ch/report/ar5/. Cambridge University Press.

Covenant of Mayors, 2010. Technical annex to the SEAP template instructions document: The emission factors.

Det Norske Veritas, 2010. Recommended practice: Design and operation of CO2 pipelines.
European Climate Foundation, 2010. Roadmap 2050 Volume 1: Technical and Economic Analysis, A Practical Guide to a Prosperous Low-Carbon Europe, Brussels.
Fimbres Weihs, G.A., Wiley, D.E., 2012. Steady-state design of CO2 pipeline networks for minimal cost per tonne of CO2 avoided. International Journal of Greenhouse Gas Control 8, 150-168.
Global Carbon Capture and Storage Institue, 2014. Global Status of CCS Report. Available from: http://www.globalccsinstitute.com/publications/global-status-ccs-february-2014
Huber, M., Ely, J.F., 1992. Prediction of Viscosity of Refrigerant and Refrigerant Mixtures. Fluid Phase Equilibrium 80, 239-248.
Huber, M., Friend, D.G., Ely, J.F., 1992. Prediction of the Thermal Conductivity of Refrigerants and Refrigerant Mixtures. Fluid Phase Equilibria 80, 249-261.
IEA, 2014. IEA's Energy Technology Perspectives 2014.
Americal Petroleum Institute, 2004. API 5L: Specifications for Line Pipe.
Jakobsen, J.P., Brunsvold, A., Husebye, J., Hognes, E.S., Myhrvold, T., Friis-Hansen, P., Hektor, E.A., Torvanger, A., 2011. Comprehensive assessment of CCS chains–Consistent and transparent methodology. Energy Procedia 4, 2377-2384.
Jakobsen, J.P., Roussanaly, S., Brunsvold, A., Anantharaman, R., 2014. A Tool for Integrated Multi-criteria Assessment of the CCS Value Chain. Energy Procedia 63, 7290-7297.
Jones, D., Cosham, A., Armstrong, K., Barnett, J., Cooper, R., 2013. Fracture Propagation Control in Dense Phase CO2 Pipelines, Proceedings of the 6th International Pipeline Technology Conference, pp. 7-9.
Knoope, M.M.J., Guijt, W., Ramírez, A., Faaij, A.P.C., 2014. Improved cost models for optimizing CO2 pipeline configuration for point-to-point pipelines and simple networks. International Journal of Greenhouse Gas Control 22, 25-46.
Knoope, M.M.J., Ramírez, A., Faaij, A.P.C., 2013. A state-of-the-art review of techno-economic models predicting the costs of CO2 pipeline transport. International Journal of Greenhouse Gas Control 16, 241-270.
Koring, K., Hoening, V., Hoppe, H., Horsch, J., Suchak, C., Klevenz, V., Emberger, B., 2013. Deployment of CCS in the Cement industry, in: IEAGHG (Ed.).
Luo, X., Wang, M., Oko, E., Okezue, C., 2014. Simulation-based techno-economic evaluation for optimal design of CO2 transport pipeline network. Applied Energy 132, 610-620.
McCoy, S.T., Rubin, E.S., 2008. An engineering-economic model of pipeline transport of CO2 with application to carbon capture and storage. International Journal of Greenhouse Gas Control 2, 219-229.
Metz, B., Davidson, O., Coninck, H.D., Loos, M., Meyer, L., 2005. Carbon Dioxide Capture And Storage: IPCC Special Report. Cambridge University Press.
Morbee, J., Serpa, J., Tzimas, E., 2012. Optimised deployment of a European CO2 transport network. International Journal of Greenhouse Gas Control 7, 48-61.
Peng, D.Y., Robinson, D.B., 1976. A new two-constant equation of state. Industrial and Engineering Chemistry Fundamentals 15, 59-64.
Rouhani, S.Z., Axelsson, E., 1970. Calculation of void volume fraction in the subcooled and quality boiling regions. International Journal of Heat and Mass Transfer 13, 383-393.
Roussanaly, S., Brunsvold, A.L., Hognes, E.S., 2014. Benchmarking of CO2 transport technologies: Part II – Offshore pipeline and shipping to an offshore site. International Journal of Greenhouse Gas Control 28, 283-299.
Roussanaly, S., Bureau-Cauchois, G., Husebye, J., 2013a. Costs benchmark of CO2 transport technologies for a group of various size industries. International Journal of Greenhouse Gas control 12C, 341–350.
Roussanaly, S., Jakobsen, J.P., Hognes, E.H., Brunsvold, A.L., 2013b. Benchmarking of CO2 transport technologies: Part I—Onshore pipeline and shipping between two onshore areas. International Journal of Greenhouse Gas Control 19C.
Selander, W.N., 1978. Explicit Formulas for the Computation of Friction Factors in Turbulent Pipe Flow. Chalk River Nuclear Laboratories, Chalk River, Ontario CANADA.
The Global CCS Institute, 2015. The Global Status of CCS 2015.

Trading Economics, 2011. Trading Economics database on Euro area inflation rate.
Wetenhall, B., Race, J.M., Downie, M.J., 2014. The Effect of CO2 Purity on the Development of Pipeline Networks for Carbon Capture and Storage Schemes. International Journal of Greenhouse Gas Control 30, 197-211.
Witkowski, A., Rusin, A., Majkut, M., Rulik, S., Stolecka, K., 2013. Comprehensive analysis of pipeline transportation systems for CO 2 sequestration. Thermodynamics and safety problems. Energy Conversion and Management 76, 665-673.
Zhao, D., Tian, Q., Li, Z., Zhu, Q., 2016. A new stepwise and piecewise optimization approach for CO2 pipeline. International Journal of Greenhouse Gas Control 49, 192-200.